# NgCAM and VAMP2 reveal that direct delivery and dendritic degradation maintain axonal polarity

Alec T. Nabb and Marvin Bentley*
Department of Biological Sciences and the Center for Biotechnology and Interdisciplinary Studies, Rensselaer Polytechnic Institute, Troy, NY 12180

**ABSTRACT** **Neurons are polarized cells of extreme scale and compartmentalization. To fulfill their role in electrochemical signaling, axons must maintain a specific complement of membrane proteins. Despite being the subject of considerable attention, the trafficking pathway of axonal membrane proteins is not well understood. Two pathways, direct delivery and transcytosis, have been proposed. Previous studies reached contradictory conclusions about which of these mediates delivery of axonal membrane proteins to their destination, in part because they evaluated long-term distribution changes and not vesicle transport. We developed a novel strategy to selectively label vesicles in different trafficking pathways and determined the trafficking of two canonical axonal membrane proteins, neuron–glia cell adhesion molecule and vesicle-associated membrane protein-2. Results from detailed quantitative analyses of transporting vesicles differed substantially from previous studies and found that axonal membrane proteins overwhelmingly undergo direct delivery. Transcytosis plays only a minor role in axonal delivery of these proteins. In addition, we identified a novel pathway by which wayward axonal proteins that reach the dendritic plasma membrane are targeted to lysosomes. These results redefine how axonal proteins achieve their polarized distribution, a crucial requirement for elucidating the underlying molecular mechanisms.**

**Monitoring Editor**
Avital Rodal
Brandeis University

Received: Aug 30, 2021
Revised: Oct 20, 2021
Accepted: Oct 25, 2021

## INTRODUCTION

Neurons are polarized cells that typically have several dendrites and a single axon to fulfill specialized functions in electrochemical signaling (Bentley and Banker, 2016). In most neurons, axons constitute the majority of the cellular volume, and most of the biosynthetic pathway is devoted to their maintenance. Axons must maintain a specific complement of membrane proteins that mediate propagation of action potentials, the release of neurotransmitters, and interaction with myelinating cells. Axonally polarized membrane proteins are manufactured in the soma and achieve their polarized distribution by selective membrane trafficking (Burack *et al.*, 2000). The initial steps of this trafficking pathway are well defined; proteins are synthesized in the rough endoplasmic reticulum and traffic through the Golgi apparatus. Subsequent steps are less clear, despite being the subject of considerable attention in the past 20 years. Progress has been made toward understanding the mechanisms that maintain polarized membrane proteins in their proper domain (Garrido *et al.*, 2001; Sampo *et al.*, 2003; Bel *et al.*, 2009; Akin *et al.*, 2015; Fletcher-Jones *et al.*, 2019). In contrast, the trafficking pathway of axonal membrane proteins from the trans-Golgi to the axon remains unclear (Burack *et al.*, 2000; Silverman *et al.*, 2001; Horton and Ehlers, 2003; Sampo *et al.*, 2003; Wisco *et al.*, 2003; Yap *et al.*, 2008a, b; Lasiecka and Winckler, 2011; Das *et al.*, 2015; Bentley and Banker, 2016). As a consequence, axonal sorting signals and the axonal sorting machinery, in contrast to those of dendritically polarized proteins (Farías *et al.*, 2012; Bonifacino, 2014; Guardia *et al.*, 2018), have not been clearly identified (Bentley and Banker, 2016).

This article was published online ahead of print in MBoC in Press (http://www.molbiolcell.org/cgi/doi/10.1091/mbc.E21-08-0425) on November 3, 2021.

Author contributions: A.T.N. designed and performed experiments, analyzed data, and wrote the manuscript; M.B. supervised the research, conceptualized the study, designed experiments, and wrote the manuscript.

Declaration of interests: The authors declare no competing interest.

*Address correspondence to: Marvin Bentley (bentlm3@rpi.edu).

Abbreviations used: NgCAM, neuron-glia cell adhesion molecule; PBS, phosphate-buffered saline; PFA, paraformaldehyde; SA, streptavidin; SBP, streptavidin-binding peptide; SigSeq, SignalSequence; VAMP2, vesicle-associated membrane protein-2.

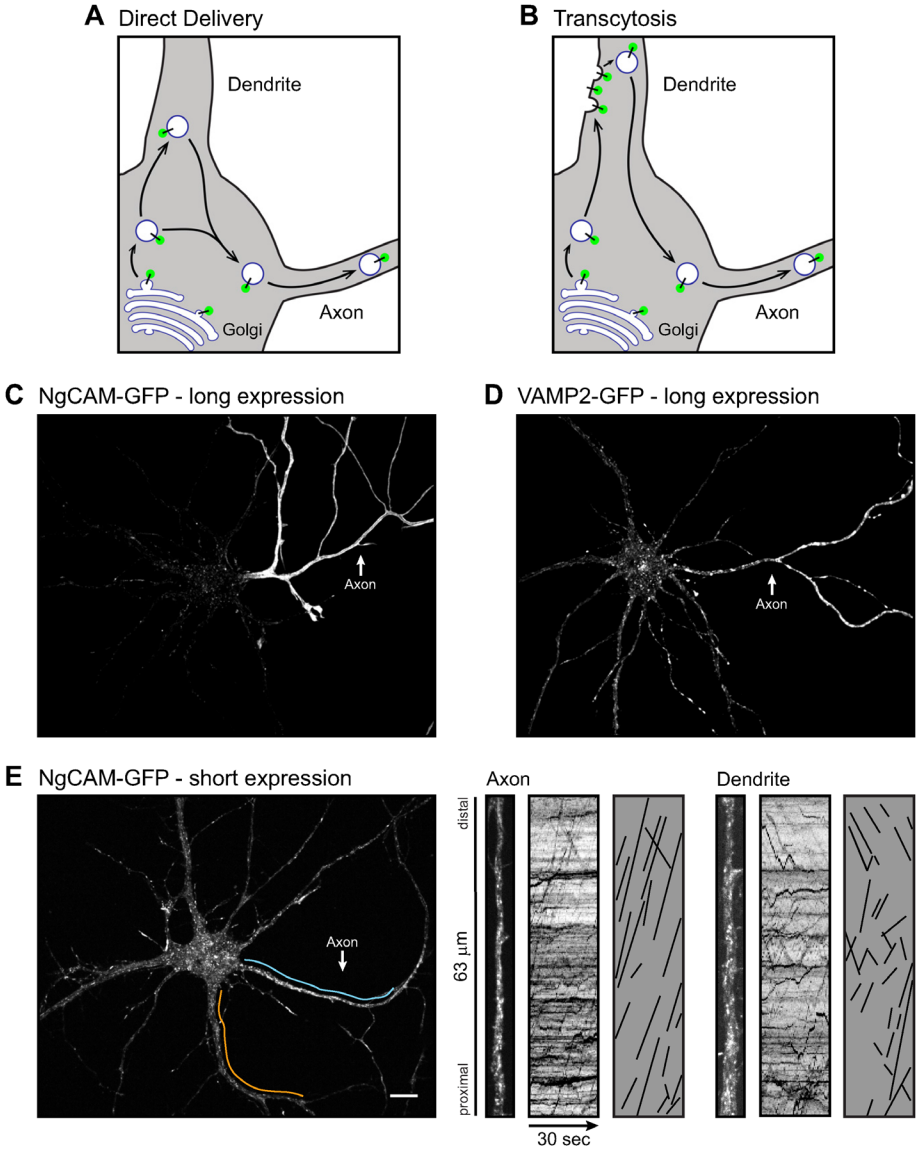


**FIGURE 1:** Maintaining the polarity of axonal membrane proteins. (A, and B) Schematics illustrating possible transport pathways for axonally polarized membrane proteins: direct delivery (A) and transcytosis (B). (C and D) Representative images of 7–9 DIV hippocampal neurons expressing NgCAM-GFP (D) or VAMP2-GFP (E) for 24 h. Both proteins accumulated in the axonal membrane. (E) Representative image of an 8 DIV hippocampal neuron expressing NgCAM-GFP for 6 h. Lines indicate sections of axon (cyan) and dendrite (orange) from which high magnification views and kymographs were generated. For clarity, transport events from kymographs are redrawn as black lines. Kymographs show that NgCAM underwent predominantly anterograde transport in the axon and bidirectional transport in the dendrite. Scale bar: 10 µm.

Two pathways by which axonal membrane proteins can reach the axon have been proposed: direct delivery and transcytosis (Winckler and Mellman, 1999). During direct delivery, axonally polarized membrane proteins are sorted into axon-selective vesicles at the trans-Golgi network (Sampo *et al.*, 2003; Fletcher-Jones *et al.*, 2019). These vesicles can enter dendrites, where they move bidirectionally, but do not fuse with the dendritic plasma membrane (Burack *et al.*, 2000; Bentley and Banker, 2016; Nabb *et al.*, 2020). Cargo proteins are delivered to the plasma membrane only after vesicles reach the axon (Figure 1A). For transcytosis, axonally polarized membrane proteins leave the Golgi in vesicles destined for the dendritic plasma membrane (Wisco *et al.*, 2003). On delivery to the dendritic membrane, proteins are rapidly endocytosed into axon-selective vesicles which deliver them to the axon (Figure 1B). The two seminal studies, both evaluating delivery of the canonical axonally polarized protein neuron–glia cell adhesion molecule (NgCAM; L1CAM in mammals) in fixed cells, came to opposite conclusions. Wisco *et al.* found that transcytosis is the primary delivery mode for axonal membrane proteins; Sampo *et al.* found that axonal membrane proteins are delivered only by direct delivery and rarely, if ever, reach the dendritic plasma membrane (Sampo *et al.*, 2003; Wisco *et al.*, 2003). To date, this controversy has not been resolved and the relative contributions of these pathways to axonal delivery are still unknown.

Here we use live-cell imaging and quantitative transport analysis of vesicles to definitively address this fundamental question. We developed a strategy to specifically label transcytotic and Golgi-derived vesicles moving in the axon and measured the transport contributions of direct delivery and transcytosis to the axonal delivery of two axonally polarized membrane proteins, NgCAM and vesicle-associated membrane protein 2 (VAMP2 or synaptobrevin 2). We found that both proteins overwhelmingly underwent direct delivery. While there was some transcytotic delivery, this plays only a minor role. In contrast to the findings in Sampo *et al.* (2003), we found that a fraction of axonal proteins reaches the dendritic plasma membrane. Instead of undergoing transcytosis, most of these targeted to lysosomes, presumably for degradation. Resolving this important question defines the trafficking framework for the polarized delivery of axonal proteins, a necessary step toward elucidating the underlying molecular mechanisms.

## RESULTS

### NgCAM and VAMP2 are polarized to the axon

To investigate axonal trafficking pathways, we focused on two canonical axonal proteins, NgCAM and VAMP2, which are polarized to the axonal plasma membrane (Jareb and Banker, 1998; Silverman *et al.*, 2001; Sampo *et al.*, 2003; Wisco *et al.*, 2003; Lewis *et al.*, 2011; Hoo *et al.*, 2016). To illustrate this localization, we expressed NgCAM-GFP (Figure 1C) or VAMP2-GFP (Figure 1D) in cultured hippocampal neurons for 24 h. As expected, both proteins were dramatically enriched in the axon. This distribution matched that of endogenous L1CAM and VAMP2 (Supplemental Figure S1). Because the bright membrane labeling obscured axonal vesicles, we used shorter expression times to visualize vesicle transport. Expression of NgCAM-GFP for shorter periods (5–11 h) produced vesicle labeling in axon and dendrites,

with minimal buildup in the plasma membrane (Figure 1E and Supplemental Video S1). Kymographs show that vesicles moved in axons and dendrites. For clarity, transport events from kymographs were redrawn as solid lines. Kymograph lines with a positive slope indicate anterograde transport and those with a negative slope indicate retrograde transport, a convention that is followed in all figures. The transport behavior exhibited by NgCAM—vesicles move bidirectionally in dendrites and have a strong bias to the axon where they undergo long-range anterograde movements—is the hallmark of axon-selective vesicle transport (Burack *et al.*, 2000; Bentley and Banker, 2016; Nabb *et al.*, 2020).

### A novel strategy to simultaneously visualize golgi-derived and endocytic vesicles

The relative contribution of each proposed pathway to delivering membrane proteins to the axon is unknown (Horton and Ehlers, 2003; Bentley and Banker, 2016). Membrane proteins are delivered by vesicle transport, a readout that is unavailable in experiments with fixed samples. Pulse-chase experiments, in which cargo proteins are retained in the ER or Golgi and released in synchrony, can address this, but are difficult to interpret because they are prone to disrupt the sorting machinery that maintains the fidelity of the endomembrane system and have given inconclusive results (Horton and Ehlers, 2003; Bentley and Banker, 2016). Live-cell imaging of vesicle transport is therefore necessary to track proteins and determine their trafficking pathway. Finally, antibody uptake assays are unable to visualize endocytic and Golgi-derived vesicles in the same cells, a necessity to assess the relative contribution of each trafficking pathway. Therefore, it is crucial to revisit this important question and develop a novel strategy—one that utilizes modern cell biological tools—to conclusively determine the trafficking pathways of axonally polarized membrane proteins.

To measure the relative contributions of direct delivery and transcytosis to axon-selective transport, we sought an approach capable of determining whether individual vesicles traveling anterograde in the axon contained proteins that had trafficked to the dendritic plasma membrane. We designed an NgCAM construct with a C-terminal GFP and a streptavidin (SA)-binding peptide (SBP) in the N-terminal ectodomain (Figure 2A). The 38-residue SBP tag binds SA with high affinity ($K_d \approx 2.5$ nM) (Keefe *et al.*, 2001; McCann *et al.*, 2005). SA cannot diffuse across the plasma membrane (McCann *et al.*, 2005) and fluorescent SA (i.e., SA conjugated to Alexa Fluor 555; SA555) in the culture medium can only bind to SBP-NgCAM-GFP if the protein has reached the cell surface. Interaction between SA and biotin is stable at a wide pH range (Morag *et al.*, 1996) and interactions are likely to remain stable throughout endocytosis and subsequent trafficking. Vesicles containing NgCAM that has previously trafficked to the dendritic plasma membrane will be labeled by both fluorescent SA and GFP, whereas vesicles that contain only NgCAM that has not been to the cell surface will be labeled only by GFP (Figure 2B). SA is a tetramer, and each subunit is conjugated to a bright fluorescent organic dye. Therefore, SA is likely to label vesicles that contain too few copies of the protein to be visualized by GFP, and we expect to see some vesicles labeled by SA alone. This strengthens the conclusion that vesicles labeled only by GFP do not contain proteins that have been exposed to the plasma membrane. This labeling strategy differentiates the origin of axonal NgCAM vesicles: vesicles that are labeled only by GFP are Golgi derived and undergoing direct delivery while vesicles that are labeled by SA arrived by way of the dendritic plasma membrane and are undergoing transcytosis. Measuring the number of vesicles in each population can quantitatively determine the contributions of each pathway.

To test the feasibility of this approach, we first confirmed that only cells expressing the SBP-tagged protein were labeled by SA555. Figure 2C shows images of two cultured hippocampal neurons. Both cells were visible by DIC, but only one expressed SBP-NgCAM-GFP. An image from the red channel shows that only the neuron expressing SBP-NgCAM-GFP was labeled with SA555. To confirm this quantitatively, we compared fluorescence measurements from three cell populations: 1) untransfected neurons, 2) neurons expressing NgCAM-GFP without an SBP tag, and 3) neurons expressing SBP-NgCAM-GFP (Figure 2, D and E). As expected, only cells expressing SBP-NgCAM-GFP exhibited SA555 fluorescence. Neither untransfected nor neurons expressing NgCAM-GFP exhibited SA555 labeling above background. Furthermore, SA555 labeling correlated with SBP-NgCAM-GFP expression (Figure 2E), indicating that the concentration of SA555 in the medium was sufficient to saturate available SBP binding sites. These findings confirmed previous studies showing the extraordinarily high specificity of SBP binding to fluorescent SA (McCann *et al.*, 2005).

Next, we determined whether addition of the SBP tag to the ectodomain of NgCAM and exposure to SA affected trafficking behavior. Long-term expression of SBP-NgCAM-GFP resulted in the same axonally polarized membrane distribution as exhibited by NgCAM-GFP (Supplemental Figure S2). As expected, SA555 in the medium interacted with SBP-NgCAM-GFP in the plasma membrane and labeled the axon. Short-term expression of SBP-NgCAM-GFP produced the same localization as NgCAM-GFP. Vesicles were distributed throughout the somatodendritic region and enriched in the axon (Figure 2C). Kymographs show that SBP-NgCAM-GFP exhibited the same distinctive transport behavior as NgCAM-GFP; vesicles underwent bidirectional transport in dendrites and predominantly anterograde transport in the axon. Transport of SBP-NgCAM-GFP was not altered by exposure to SA555. Quantification of NgCAM transport confirmed that all conditions exhibited typical axon-selective transport (Figure 2, F and G).

### NgCAM reaches the axon by direct delivery

We used this approach to determine if exposure to SA555 and subsequent washout resulted in a pulse of transcytotic SBP-NgCAM-GFP in the axon. Eight hours after transfection, neurons were exposed to SA555 for 30 min, followed by washout and live-cell imaging within 30 to 360 min (Figure 3A). Vesicles labeled with GFP and not SA555 (i.e., directly delivered carriers) moved anterograde in the axon consistently throughout the time course, indicating that expression had reached a steady state before SA555 was added (Figure 3B). Retrograde transport of GFP-labeled vesicles was similarly consistent throughout (Figure 3C).

Starting at 90 min after washout, there were SA555-labeled vesicles moving anterograde. However, these consistently represented a relatively small fraction of all anterograde vesicles, indicating that while transcytosis occurs, it plays a minor role in comparison to direct delivery (Figure 3D).

Analysis of the retrograde movement of SA555-labeled vesicles showed that this occurred earlier than anterograde, reaching a plateau 60 min after washout (Figure 3E). Because the plateau of SA555-labeled retrograde transport preceded the increase in SA555-labeled anterograde transport by 30+ min, and vesicles commonly underwent reversals, it is likely that a significant portion of the SA555-labeled vesicles moving anterograde at later time points were the product of axonal endocytosis and not transcytosis from dendrites. To avoid analyzing vesicles that were the product of axonal endocytosis and potentially biasing the data toward

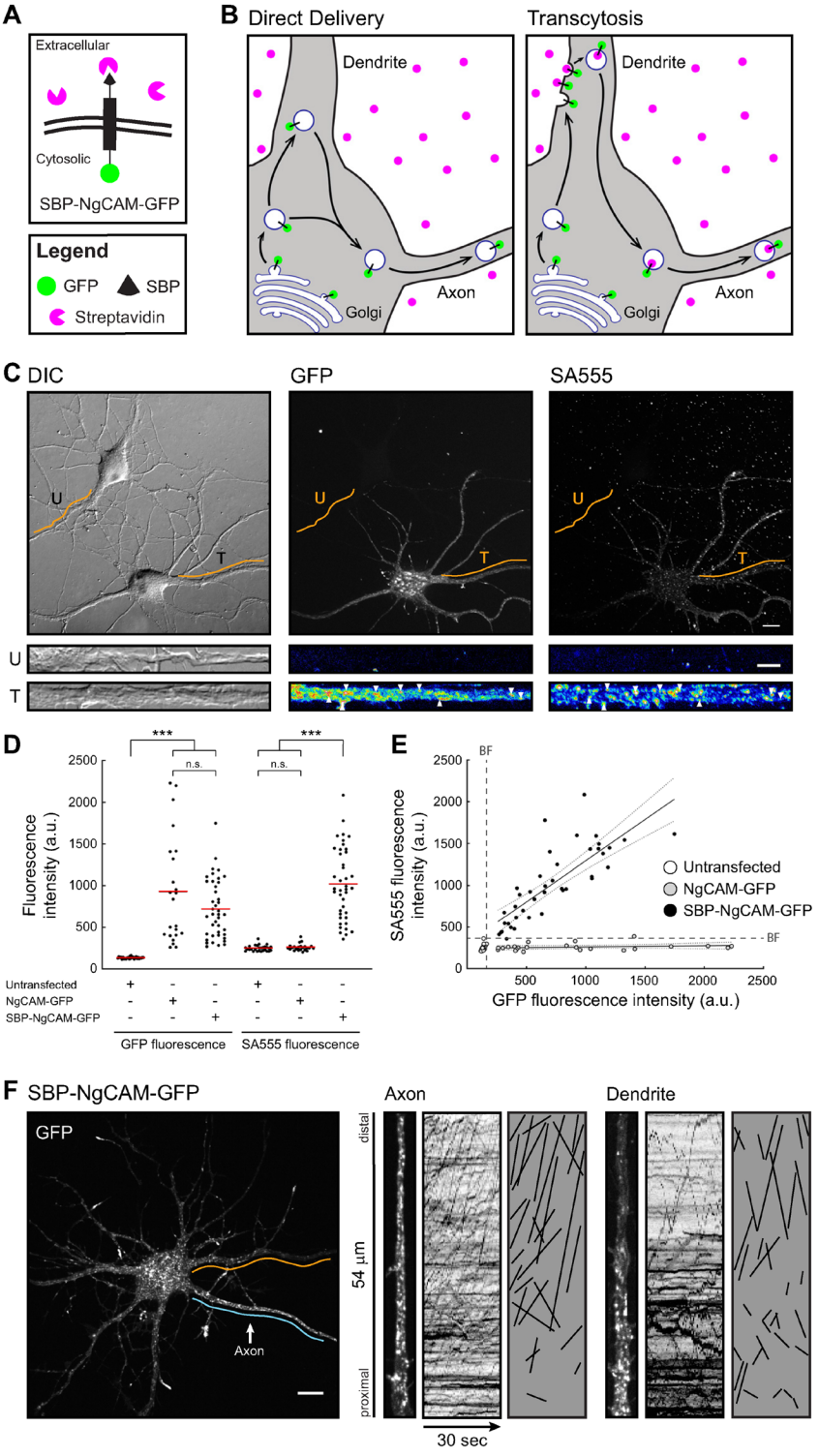


**FIGURE 2:** A novel labeling strategy differentiates golgi-derived and endocytic vesicles. (A and B) A schematic illustrating the assay to differentially label axonal vesicles undergoing direct delivery and transcytosis. NgCAM is designed with an SBP in the ectodomain and a C-terminal GFP (A). SBP-NgCAM-GFP only binds fluorescent SA after plasma membrane insertion. Axonal vesicles undergoing direct delivery are labeled by GFP only. Axonal vesicles undergoing transcytosis are also labeled by fluorescent SA (B). (C) Representative images of two 7 DIV hippocampal neurons that are untransfected (top) or expressing SBP-NgCAM-GFP (bottom). Both were incubated with SA555. Orange lines indicate a section of dendrite from which high magnification views of the untransfected (U) and transfected (T) cells were generated. Only the neuron expressing SBP-NgCAM-GFP was labeled by SA555, which colocalized with GFP-labeled endosomes (arrowheads). Scale bars: low magnification, 10 µm; high magnification, 5 µm. (D and E) Quantification of GFP and SA555 intensities in untransfected neurons, neurons expressing NgCAM-GFP, and neurons expressing SBP-NgCAM-GFP, each incubated with SA555. Only neurons expressing SBP-NgCAM-GFP exhibited SA555 labeling (D). The red line indicates the mean. SA555 labeling correlated with SBP-NgCAM-GFP expression levels (E). Black lines indicate linear fit and dotted lines indicate a 95% confidence interval. Dashed lines indicate background fluorescence (BF). Untransfected: 28 cells; NgCAM-GFP: 23 cells; SBP-NgCAM-GFP: 41 cells. (F) Representative image of an 8 DIV hippocampal neuron expressing SBP-NgCAM-GFP. Lines indicate sections of axon (cyan) and dendrite (orange) from which high magnification views and kymographs were generated. For clarity, transport events from kymographs are redrawn as black lines. Kymographs from the GFP channel show that SBP-NgCAM-GFP underwent predominantly anterograde transport in the axon and bidirectional transport in the dendrite. Scale bar: 10 µm. (G) Quantification of NgCAM transport events. NgCAM-GFP, SBP-NgCAM-GFP, and SBP-NgCAM-GFP + SA555 exhibited the same transport behavior. NgCAM-GFP: 1447 events in 19 cells. SBP-NgCAM-GFP: 1705 events in 21 cells. SBP-NgCAM-GFP and SA555: 1802 events in 24 cells.

transcytotic events, we focused subsequent analysis on the first 90 min after SA555 washout.

Next, we carefully measured the contributions of direct delivery and transcytosis to axonal NgCAM delivery (Figure 4). We expressed SBP-NgCAM-GFP in neurons for 5–11 h and incubated cells with SA555 for 30 min, followed by a rinse to remove unbound SA and live-cell imaging within 90 min of SA555 washout. GFP-labeled vesicles (total NgCAM) exhibited the same distribution as before (Figure 4A and Supplemental Video S2). Vesicles were polarized to the axon where they underwent long-range anterograde transport (Figure 4B). SA555-labeled vesicles (endocytosed

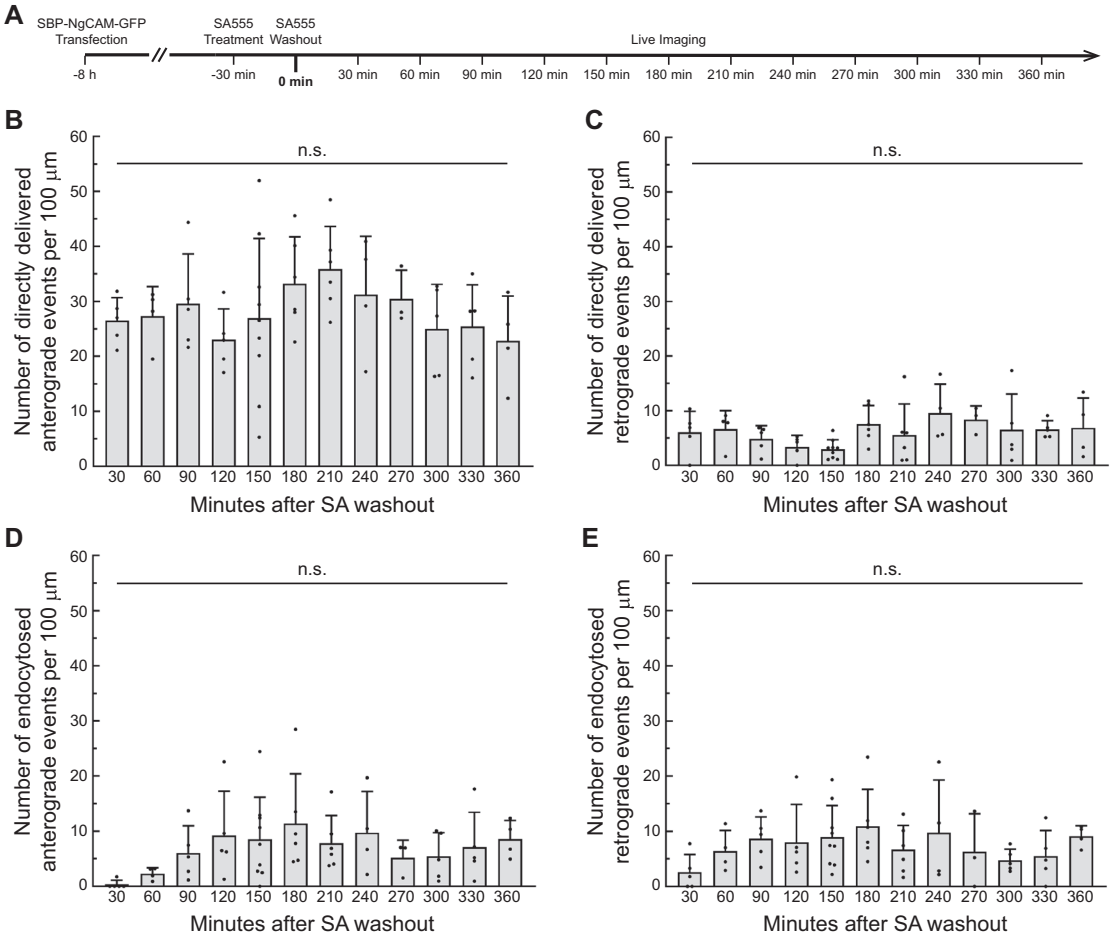


**FIGURE 3:** Transcytotic NgCAM delivery to axons plateaus at a low level. (A) A schematic showing the experimental design. Eight hours after transfection with SBP-NgCAM-GFP, neurons were treated with SA555 for 30 min and imaged at various time points after SA555 washout. (B–E) Quantification of axonal transport events. Anterograde transport events labeled by GFP (B). Retrograde transport events labeled by GFP (C). Anterograde transport events labeled by SA555 (D). Retrograde transport events labeled by SA555 (E). Data from 61 cells; n.s., no statistical significance.

NgCAM) were less abundant overall (Figure 4A). High magnification images revealed endocytosed NgCAM in dendrites consistent with previous literature (Wisco *et al.*, 2003). In contrast to the axonally polarized distribution of total NgCAM, endocytosed NgCAM vesicles were evenly distributed throughout the cell. Kymographs show that endocytosed NgCAM vesicles were mostly stationary in dendrites (Figure 4B). This was in striking contrast to the dynamic behavior of total NgCAM. NgCAM-GFP expression also labels comparable stationary vesicles in dendrites, confirming that these are not caused by interaction with SA555 (Figure 1F). In the axon, SA555-labeled vesicles were either stationary or underwent retrograde movements (Figure 4B). Anterograde transport of endocytosed NgCAM in the axon was rare. We used kymograph analysis to quantitatively evaluate the transport behavior of axonal NgCAM and evaluated total NgCAM and endocytosed NgCAM separately (Figure 4C). There were vastly more anterograde GFP than SA555 transport events in the axon; the ratio of anterograde GFP to SA555 transport events in the axon was 23.6 to 1 (Figure 4C).

In addition to the vast difference in the total number of total NgCAM vesicles compared with endocytosed NgCAM vesicles, we noticed that these two populations exhibited different transport parameters. To evaluate this, we measured the run lengths and velocities of total NgCAM, endocytosed NgCAM, and directly delivered NgCAM (i.e., vesicles labeled by GFP but not SA555) in the axon (Figure 4, D and E). Directly delivered NgCAM displayed significantly higher anterograde run lengths and velocities than endocytosed NgCAM. This was in contrast to retrograde events, which exhibited homogenous transport parameters. The differences in anterograde movements suggest that directly delivered NgCAM vesicles that enter the axon are substantively different from transcytotic vesicles containing endocytosed NgCAM.

We next asked whether these two vesicle populations underwent different transport behaviors in the proximal axon. The proximal axon consists of three distinct regions. The first 10–20 µm stain for MAP2 and have dendritic characteristics (Caceres *et al.*, 1984; Hedstrom *et al.*, 2008; Yamamoto *et al.*, 2012; Leterrier and Dargent, 2014; Petersen *et al.*, 2014; Gumy *et al.*, 2017). This is followed by the axon initial segment, which contains a high concentration of voltage-gated channels (Huang and Rasband, 2018; Leterrier, 2018), a specialized cytoskeleton (Leterrier *et al.*, 2017), and marks the boundary for dendritic vesicles (Burack *et al.*, 2000; Al-Bassam *et al.*, 2012; Jenkins *et al.*, 2012; Jensen *et al.*, 2014; Petersen *et al.*, 2014; Yang *et al.*, 2019; Radler *et al.*, 2020). Beyond the initial segment, the axon is relatively homogenous and extends long distances. Axonal vesicles exhibit the same transport parameters throughout these regions, unencumbered by the cytoskeletal differences. To determine any differences in how vesicles traversed the proximal axon, we measured transport events depending on where

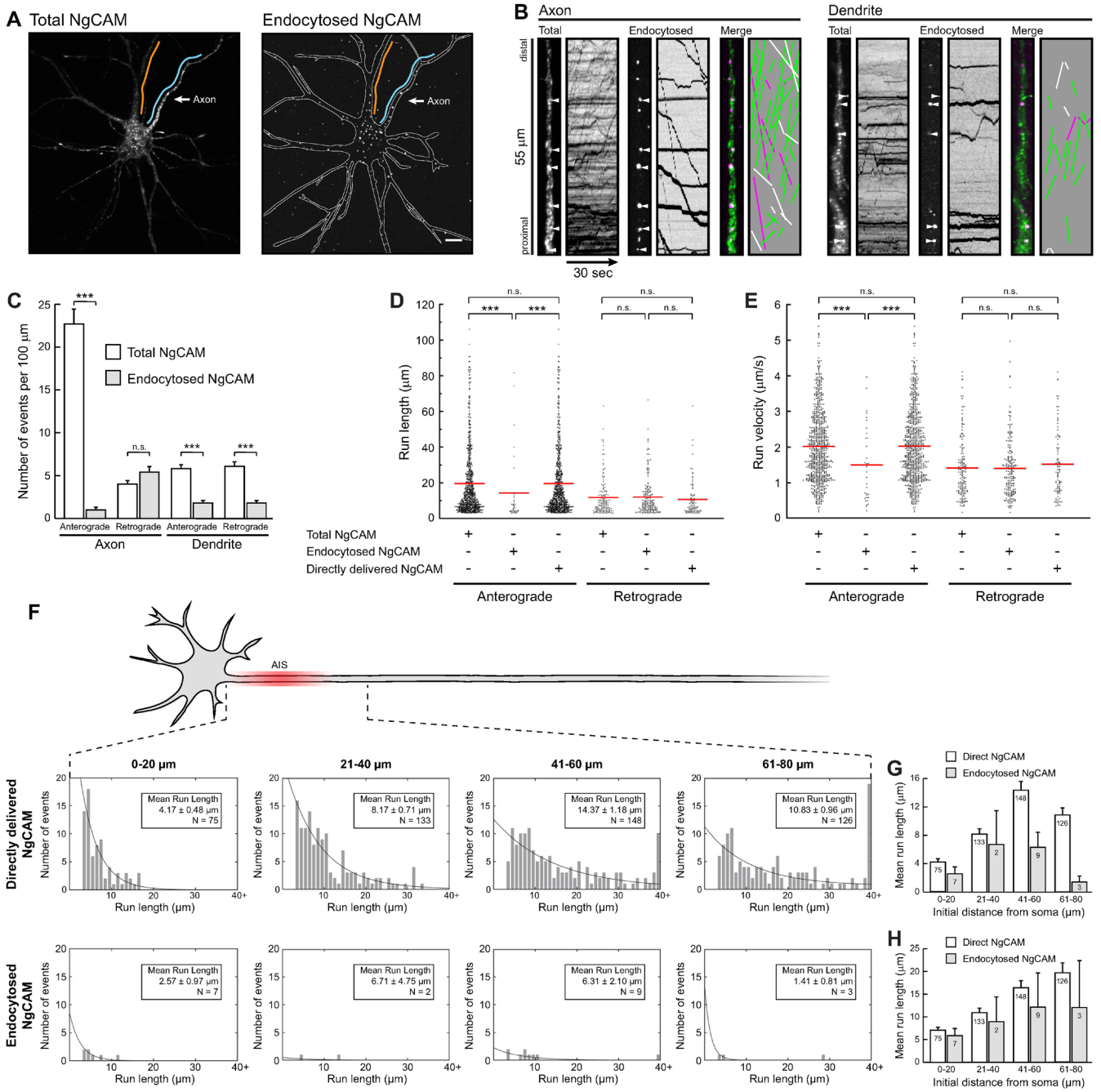


FIGURE 4: Axonal NgCAM is directly delivered. (A and B) Representative images of an 8 DIV neuron expressing SBP-NgCAM-GFP and incubated with SA555 (A). Total NgCAM was visualized by GFP (left) and endocytosed NgCAM by SA555 (right). Lines indicate sections of axon (cyan) and dendrite (orange) from which high magnification views and kymographs were generated. Scale bar: 10 µm. High magnification images and kymographs of total and endocytosed NgCAM (B). Arrowheads in high magnification images point to examples of endocytic structures labeled by both GFP and SA555. Transport events from kymographs are redrawn as colored lines (overlapping events are white; events visualized by GFP only are green; events visualized by SA555 only are magenta). Kymographs show that most GFP-labeled vesicles trafficking anterograde in the axon were not labeled by SA555. SA555-labeled large structures that moved retrograde in the axon and were predominantly stationary in dendrites. (C–E) Quantification of NgCAM transport events (C). Endocytosed NgCAM vesicles exhibited decreased anterograde run lengths (D) and velocities (E) in the axon. Total NgCAM: all GFP-labeled vesicles; endocytosed NgCAM: all SA555-labeled vesicles; directly delivered NgCAM: all GFP-labeled vesicles not also labeled by SA555. Red lines show the mean. (F–H) Quantification of NgCAM transport in the proximal axon (F). Transport events in axons were binned into four 20-µm segments, indicated by the distance to the soma. Each anterograde transport event was assigned to the bin corresponding to the starting position. Run lengths of vesicles labeled by GFP only (Directly Delivered) and SA555 (Endocytosed) are shown as histograms for each bin. Reported means were generated from the fit of the histogram (F). Inserts show means run lengths from the fit of the histogram. Bar graph showing mean run lengths from the fit of the histograms (G). Bar graph showing arithmetic mean (H). Data from 24 cells. Total NgCAM: 1802 events; endocytosed NgCAM: 494 events.

in the axon transport was initiated. Anterograde transport events were assigned to the 20-µm axon segment in which transport was initiated during recording (Figure 4, F–H). Directly delivered NgCAM vesicles exhibited longer run lengths than vesicles containing endocytic NgCAM. This was most pronounced in the distal sections, where directly delivered vesicles routinely underwent excursions that were longer than 40 µm. No movement of more than 30 µm was recorded for endocytosed NgCAM. These results show that endocytosed vesicles rarely move beyond the initial segment, the region of the axon where movement of dendritic vesicles ends (Petersen *et al.*, 2014; Bentley and Banker, 2016; Gumy and Hoogenraad, 2018; Radler *et al.*, 2020; Koppers and Farías, 2021).

Taken together, these data show that the overwhelming majority of NgCAM delivered to the axon, approximately 96% of vesicles, uses the direct delivery pathway to reach the axon. Axonal vesicles that carry endocytosed NgCAM exhibit different transport behavior and rarely reach the distal axon, possibly due to a different complement of motor proteins.

### VAMP2 reaches the axon by direct delivery

We next applied the strategy to quantify the trafficking of VAMP2. VAMP2 constructs with a fluorescent protein in the C-terminal ectodomain are well characterized and have been used in a range of experiments (Ahmari *et al.*, 2000; Sankaranarayanan and Ryan, 2000; Sampo *et al.*, 2003; Lewis *et al.*, 2011; Liu *et al.*, 2012; Gumy *et al.*, 2017). Addition of an SBP C-terminal to the GFP construct is therefore unlikely to affect trafficking. This was confirmed when we expressed VAMP2-GFP-SBP in hippocampal neurons and treated cells with SA555 as described above (Figure 5A and Supplemental Video S3). GFP-labeled VAMP2 vesicles were distributed throughout dendrites and enriched in the axon. In the axon, GFP-labeled vesicle transport exhibited a strong anterograde bias (Figure 5B), similar to axonal NgCAM transport. Endocytosed VAMP2, visualized with SA555, was mostly localized to dendrites where it labeled bright stationary structures and a few dim vesicles that moved bidirectionally (Figure 5B). SA555 labeled few vesicles in the axon and these fell into three categories: 1) bright stationary structures, 2) bright vesicles moving retrograde, and 3) dim vesicles moving anterograde. Notably, most SA555-labeled structures were in the proximal axon with few beyond the axon initial segment. Quantitative transport analysis found that most VAMP2 vesicles entering the axon underwent direct delivery (Figure 5C).

Similar to NgCAM, we noticed a difference between the transport of SA555-labeled vesicles in the proximal and distal axon. Anterograde vesicles undergoing direct delivery exhibited increased run lengths and velocities compared with vesicles containing endocytosed VAMP2 (Figure 5, D and E). There was no difference in retrograde transport. Analysis of transport in the proximal axon again showed that little anterograde VAMP2 transport occurred beyond the first 60 µm of axon (Figure 5, F–H).

We also noticed that most SA555-labeled vesicles in the distal axon were dim, barely visible above background. This was surprising because Alexa Fluor 555 is a bright organic dye. Bright vesicles were sparse and underwent mostly retrograde transport. The fact that the SA555 dye is a bright label and typically labels bright endocytic vesicles suggested that dim vesicles contained only a nominal number of endocytosed VAMP2 proteins. To verify this observation, we quantified the intensities of motile SA555-labeled vesicles in the distal axon. This analysis confirmed that all bright vesicles underwent retrograde transport while vesicles moving anterograde were dim (Figure 5I). This observation revealed a weakness of kymograph analyses where all transport events are scored the same, regardless of the fluorescence intensity of the vesicles. Dim vesicles likely contain few copies of the protein relative to bright vesicles. Therefore, our results are consistent with the interpretation that axonal VAMP2 vesicles moving anterograde contained less endocytosed VAMP2 than those that move retrograde.

The ratio of anterograde GFP to SA555 VAMP2 vesicle transport was about 6 to 1 in the axon (Figure 5), indicating that approximately 85% of VAMP2 vesicles use the direct delivery pathway to the axon. From these results, we concluded that direct delivery is the primary trafficking pathway for axonal VAMP2.

### NgCAM and VAMP2 use the same direct delivery pathway to reach the axon

NgCAM and VAMP2 are structurally and functionally unrelated, yet both use direct delivery to reach the axon, and our analyses showed that both vesicles behaved similarly. This raises an important question: do neurons maintain multiple direct delivery pathways to the axon? Previously, NgCAM and VAMP2 were thought to utilize different trafficking pathways (Sampo *et al.*, 2003). To address this question directly, we coexpressed NgCAM-mCherry and VAMP2-GFP in the same cells (Figure 6A and Supplemental Video S4). High magnification images show that both constructs labeled many of the same vesicles in axons and dendrites (Figure 6B). Kymographs confirmed that these two proteins underwent cotransport. Quantification of the transport behavior of each vesicle population confirmed that coexpression of the two proteins together did not impact their trafficking behavior (Figure 6C). Both proteins exhibited transport behaviors comparable to when each is expressed alone. Quantification of cotransport found substantial overlap of NgCAM and VAMP2, irrespective of the direction of transport in both axons and dendrites (Figure 6D).

Next, we sought a separate method to confirm that the axonal vesicles containing NgCAM and VAMP2 were Golgi derived. For this experiment, we used a SignalSequence (SigSeq)-mCherry construct. This construct consists of the signal sequence from neuropeptide-Y fused to mCherry and labels the lumen of Golgi-derived vesicles (El Meskini *et al.*, 2001; Kaech *et al.*, 2012b; Das *et al.*, 2013; Ganguly *et al.*, 2015, 2017). Vesicle fusion with the plasma membrane releases the luminal mCherry into the culture medium. Due to the low transfection efficiency (~1% of neurons in low-density culture), secreted mCherry in the culture medium remains at negligible concentrations throughout the experiments. Therefore, vesicles labeled by SigSeq-mCherry cannot be endocytic. We coexpressed this construct with NgCAM-HaloTag that was visualized with JF647 (Grimm *et al.*, 2015) and VAMP2-GFP. As expected, SigSeq-mCherry labeled punctate vesicles throughout the neuron (Figure 6E). Kymographs demonstrate extensive cotransport of all three proteins in the axon (Figure 6F). Kymograph analysis showed that 80% of moving vesicles containing both NgCAM and VAMP2 also contained SigSeq-mCherry (Figure 6G). This shows that axonal delivery of membrane proteins is mediated by Golgi-derived vesicles that undergo direct delivery to the axon through a unified delivery pathway.

### Dendritically endocytosed axonal membrane proteins are directed to lysosomes

After finding that most endocytic NgCAM and VAMP2 vesicles in dendrites are not targeted to the axon, we sought to determine their fate. These vesicles were large, stationary, and concentrated in the soma and proximal dendrites, resemblant of mature acidified lysosomes (Farías *et al.*, 2017; Goo *et al.*, 2017; Yap *et al.*, 2018). This observation suggested that missorted axonal proteins delivered

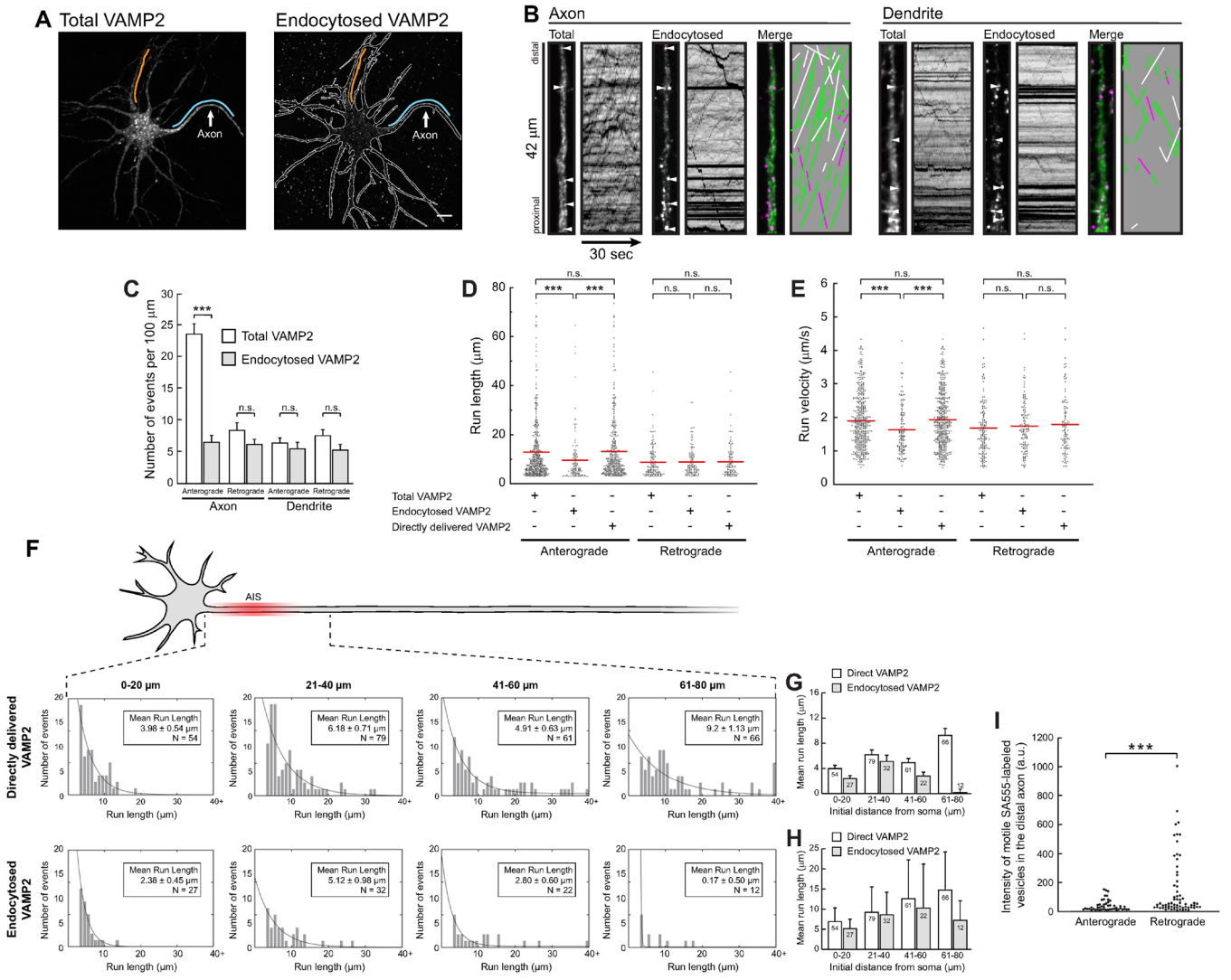


FIGURE 5: Axonal VAMP2 is directly delivered. (A and B) Representative images of an 8 DIV neuron expressing VAMP2-GFP-SBP and incubated with SA555 (A). Total VAMP2 was visualized by GFP (left) and endocytosed VAMP2 by SA555 (right). Lines indicate sections of axon (cyan) and dendrite (orange) from which high magnification views and kymographs were generated. Scale bar: 10 µm. High magnification images and kymographs of total and endocytosed VAMP2 (B). Arrowheads in high magnification images point to examples of endocytic structures labeled by both GFP and SA555. Transport events from kymographs are redrawn as colored lines (overlapping events are white; events visualized by GFP only are green; events visualized by SA555 only are magenta). Kymographs show that most GFP-labeled vesicles trafficking anterograde in the axon were not labeled by SA555. (C–E) Quantification of VAMP2 transport events. Endocytosed VAMP2 vesicles exhibited decreased anterograde run lengths (D) and velocities (E) in the axon. One directly delivered event (6.4 µm/s) was included in the analysis but not the graph (E). Total VAMP2: all GFP-labeled vesicles; Endocytosed VAMP2: all SA555-labeled vesicles; Directly Delivered VAMP2: all GFP-labeled vesicles not also labeled by SA555. Red lines show the mean. (F–H) Quantification of VAMP2 transport in the proximal axon. Transport events in axons were binned into four 20 µm segments, indicated by the distance to the soma. Each anterograde transport event was assigned to the bin corresponding to the starting position. Run lengths of vesicles labeled by GFP only (Directly Delivered) and SA555 (Endocytosed) are shown as histograms for each bin. Reported means were generated from the fit of the histogram (F). Inserts show means run lengths from the fit of the histogram. Bar graph showing mean run lengths from the fit of the histograms (G). Bar graph showing arithmetic mean (H). Data from 23 cells. Total VAMP2: 1517 events; endocytosed VAMP2: 904 events. (I) Fluorescence intensity measurements of moving SA555-labeled transport vesicles in the distal axon.

to the dendritic plasma membrane are retrieved by endocytosis and then targeted to lysosomes for degradation. To test this hypothesis, we expressed SBP-NgCAM-GFP or VAMP2-GFP-SBP, labeled their endocytic fraction with SA555, and visualized lysosomes with lysotracker (Figure 7). High magnification images of dendrites show that both endocytosed NgCAM and endocytosed VAMP2 colocalized extensively with lysosomes (Figure 7, A and B). Kymographs show overlap of each endocytosed population with lysotracker in large, stationary structures. A small population of lysotracker-negative endocytic vesicles exhibited bidirectional movement in dendrites. These were likely part of the small transcytotic pool we observed or nascent endosomes trafficking to lysosomes.

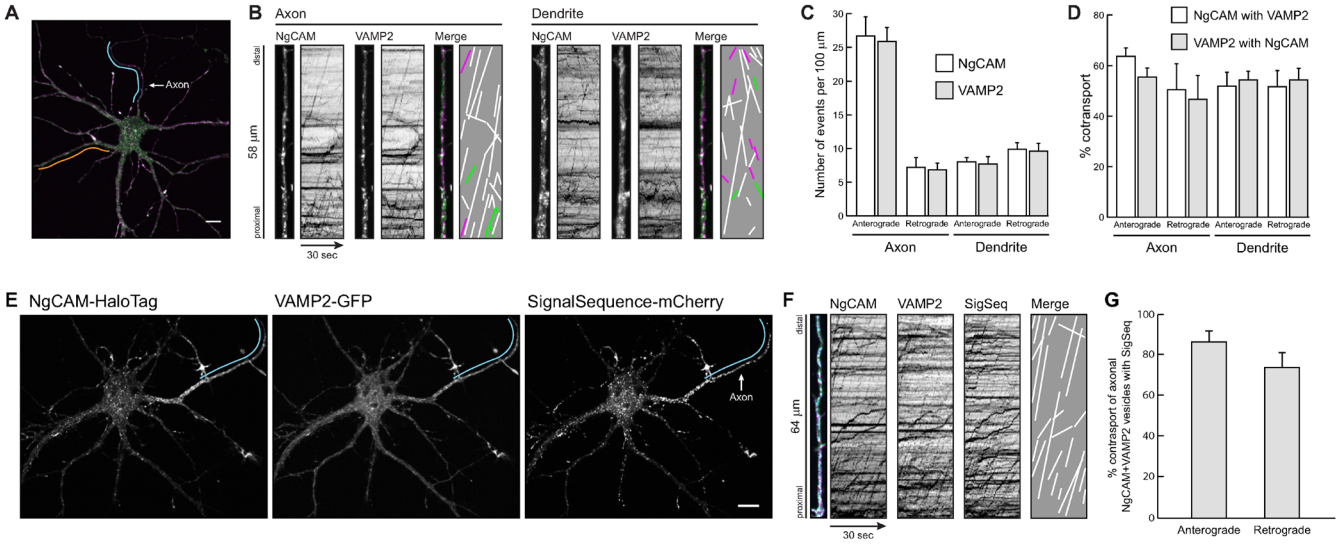


**FIGURE 6:** NgCAM and VAMP2 use the same direct delivery pathway. (A and B) Representative image of a 7 DIV neuron expressing NgCAM-mCherry and VAMP2-GFP (A). Lines indicate sections of axon (orange) and dendrite (cyan) from which high magnification views and kymographs were generated. For clarity, a subset of transport events from kymographs are redrawn as colored lines (overlapping events are white; nonoverlapping NgCAM events are magenta; nonoverlapping VAMP2 events are green) (B). Scale bar: 10 µm. (C and D) Quantification of transport of NgCAM and VAMP2 (C). Quantification of NgCAM-mCherry and VAMP2-GFP cotransport (D). Data from 15 cells. NgCAM: 1493 events; VAMP2: 1424 events. (E and F) Representative images of a 9 DIV hippocampal neuron expressing NgCAM-HaloTag, VAMP2-GFP, and SigSeq-mCherry. NgCAM-HaloTag was visualized with JF647 (A). A cyan line indicates the section of axon from which the high magnification view and kymographs were generated. For clarity, a subset of transport events overlapping in all three channels are redrawn as white lines (F). Most anterograde transport events were labeled by all three constructs. Scale bar: 10 µm. (G) Quantification of the percentage of motile vesicles in the axon that contain both NgCAM and VAMP2 and overlap with SigSeq-mCherry. Data from 11 cells. NgCAM: 632 events; VAMP2: 528 events; SigSeq-mCherry: 610 events.

To determine the extent of endocytosed vesicle targeting, we quantified the colocalization of SA555-labeled vesicles with lysotracker in dendrites (Figure 7C). The quantification showed that 67% of endocytosed NgCAM and 71% of endocytosed VAMP2 colocalized with lysotracker in dendrites. It is possible that a significant fraction of the remaining vesicles represents a pool that has not yet reached lysosomes. Finally, we asked if endogenous L1CAM and VAMP2 were found in lysosomes, as predicted by the experiment with exogenous proteins. Immunofluorescence experiments found that both endogenous L1CAM and endogenous VAMP2 colocalized with the lysosomal marker LAMP1-GFP in dendrites (Figure 7D).

These results indicate that the presence of endocytosed axonal proteins in dendrites is not evidence of a secondary mechanism for axonal delivery. Instead, they point to a fail-safe mechanism that retrieves wayward axonal proteins from the dendritic plasma membrane and subsequently targets them to lysosomes for degradation.

## DISCUSSION

In this study, we addressed a long-standing question in neuronal cell biology. We determined the trafficking pathway by which axonally polarized membrane proteins are delivered to their destination. Our results define a new model in which two separate mechanisms work in concert to maintain axonal polarity. Proteins are sorted into axon-selective transport vesicles at the Golgi and reach the axon by direct delivery. These vesicles can move in dendrites but preferentially enter the axon to deliver their cargo. A second mechanism maintains polarity by retrieving wayward axonal proteins from the dendritic plasma membrane. These proteins are endocytosed and targeted to lysosomes for degradation. This model defines a new framework that will inform future studies addressing the molecular mechanisms that maintain axonal polarity (Figure 8).

### Estimating the relative contributions of trafficking pathways

The ability to track endocytic and Golgi-derived vesicles and measure their transport in live neurons allowed us to generate a quantitative model that estimates the relative contributions of each trafficking pathway. Most vesicles reach the axon by direct delivery (i.e., without fusing with the dendritic membrane en route to the axon) based on their lack of SA label: 85% of VAMP2 and 94% of NgCAM. The remainder, 6–15%, undergoes transcytosis from the dendritic plasma membrane. Thus, direct delivery is the primary pathway for axonally polarized membrane proteins.

Axonal proteins that reach the dendritic membrane and undergo endocytosis can be rerouted to the axon or targeted to lysosomes. Estimating the prevalence of these two pathways is less straightforward, as it requires an estimate of the total available endocytosed pool. Retrograde transport of SA-labeled vesicles in dendrites is a reasonable estimate for total endocytosed vesicles because a vesicle must travel retrograde to reach the soma before it can be directed into the axon. We found an average density of about two endocytosed NgCAM and about five VAMP2 vesicles moving retrograde in each dendrite. Assuming a typical cultured hippocampal neuron has five dendrites (a conservative estimate) and that the retrograde vesicles from all dendrites enter the single axon, one would expect the total sum of endocytic vesicles undergoing anterograde transport in the axon to be ~10 for NgCAM and ~26 for VAMP2. In fact, only about one SA-labeled NgCAM and four SA-labeled VAMP2 vesicles were observed moving anterograde in the axon. Thus, only a small fraction of the dendritic vesicles containing

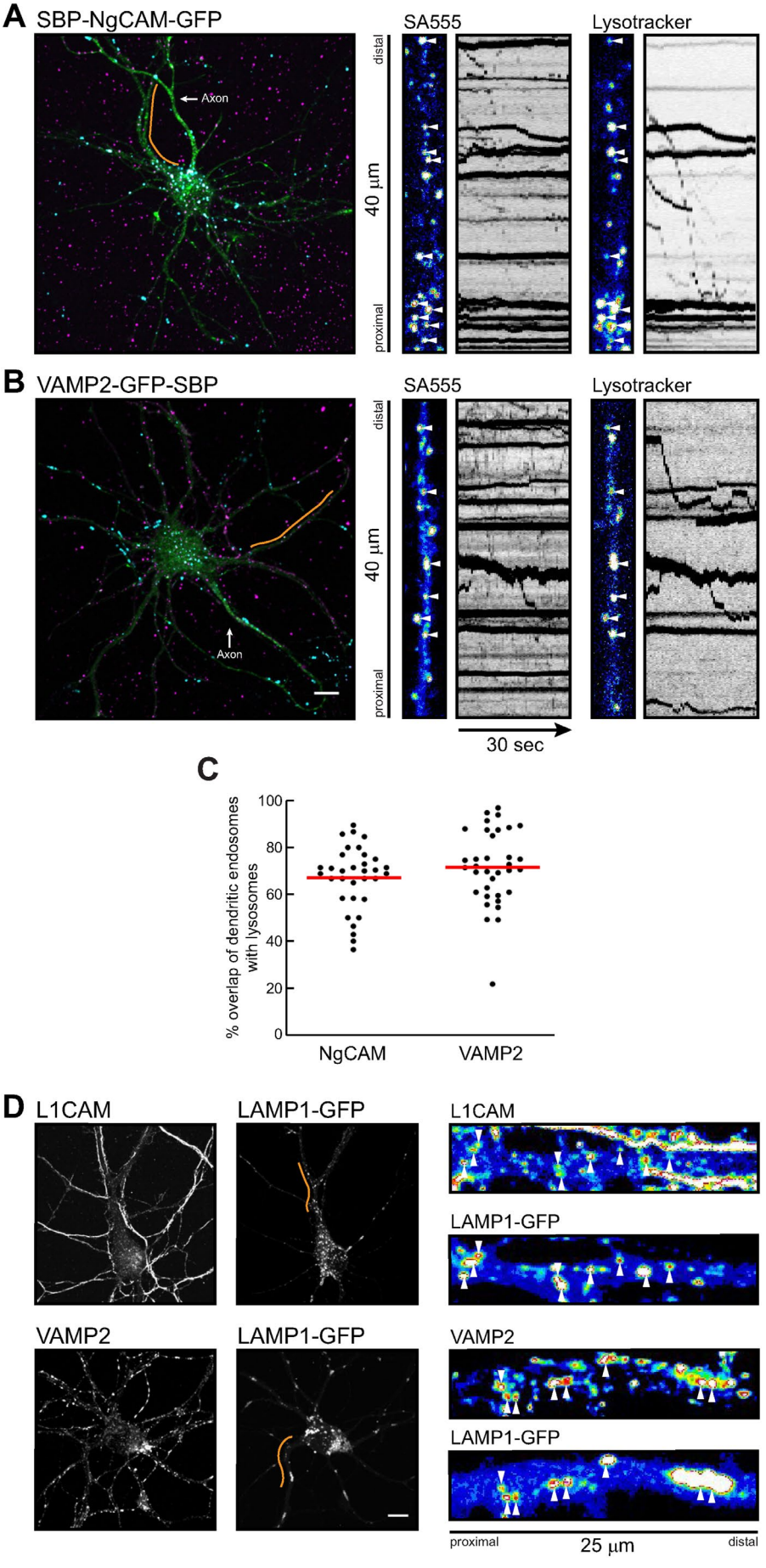


endocytosed protein (~10% for NgCAM and ~16% for VAMP2) reach the axon by transcytosis. The remainder of dendritically endocytosed vesicles (84–90%) are therefore delivered to dendritic or somatic lysosomes for degradation. It is important to note that these are rough estimates based on reasonable but unproven assumptions. However, they give a realistic sense of the relative prevalence of each pathway. These results support the hypothesis that the vast majority of axonally polarized membrane proteins undergo direct delivery and that most proteins that reach the dendritic plasma membrane are degraded in lysosomes.

### Axonally polarized membrane proteins use a single direct delivery pathway to reach the axon

One surprising outcome from this study is that both NgCAM and VAMP2 use the same direct delivery pathway to reach the axon. These proteins are vastly disparate in their structure and function. NgCAM is a type I transmembrane protein with a large ectodomain and functions as a cell adhesion molecule (Grumet, 1992). In contrast, VAMP2 is a type II transmembrane protein with a small ectodomain and a cytoplasmic SNARE motif (Sollner *et al.*, 1993; Trimble, 1993).

Previous studies that used antibody uptake and fixed specimens to determine the trafficking of NgCAM were inconclusive (Sampo *et al.*, 2003; Wisco *et al.*, 2003). Wisco *et al.* (2003) identified endocytic NgCAM vesicles in dendrites and proposed that these

**FIGURE 7:** NgCAM and VAMP2 are endocytosed into dendritic lysosomes. (A and B) Representative images of 7–8 DIV hippocampal neurons expressing SBP-NgCAM-GFP (A) or VAMP2-GFP-SBP (B), each incubated with SA555 and lysotracker deep red. Orange lines indicate sections of dendrite from which high magnification views and kymographs were generated. Arrowheads in high magnification images point to examples of endocytosed NgCAM or VAMP2 that colocalized with acidified lysosomes. Scale bar: 10 µm. (C) Quantification of colocalization between endocytosed NgCAM or VAMP2 and acidified lysosomes. Red lines show mean. Data from 25 cells. NgCAM: 12 cells, 730 endosomes; VAMP2: 13 cells, 1453 endosomes. (D) Representative images of 8 DIV neurons expressing LAMP1-GFP and stained for L1CAM or VAMP2. Orange lines indicate sections of dendrite from which high magnification views were generated. Arrowheads in high magnification images point to examples of L1CAM or VAMP2 that colocalized with LAMP-1-labeled lysosomes. Scale bar: 10 µm.

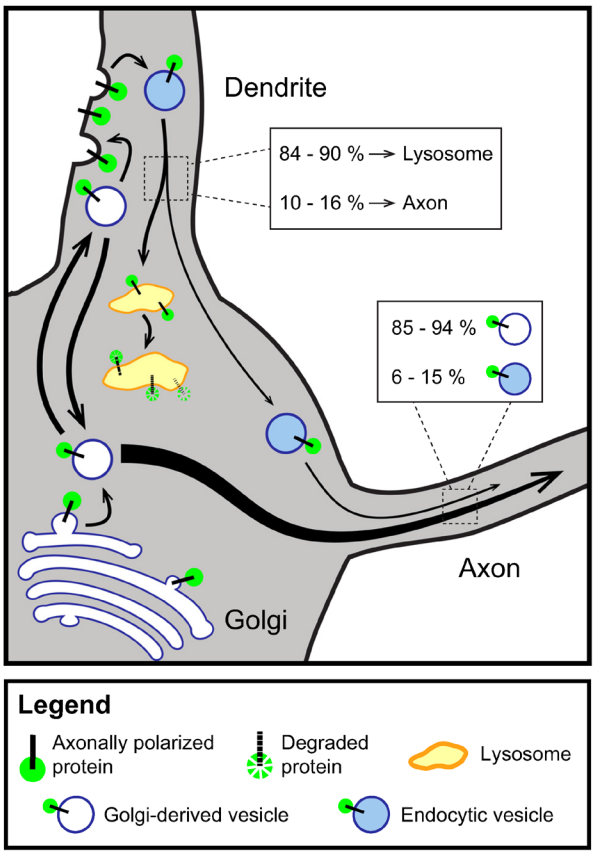


**FIGURE 8:** Direct delivery and dendritic degradation Work in concert to maintain axonal polarity. (A) A schematic illustrating the trafficking of axonally polarized membrane proteins. Most proteins reach the axon by direct delivery (85–94%). Axonal membrane proteins that reach the dendritic membrane undergo rapid endocytosis and enter one of two pathways. Most (84–90%) are targeted to lysosomes. Only 10–16% of endocytosed proteins undergo transcytosis and subsequent axonal delivery.

constituted an intermediate step of transcytosis. Sampo *et al.* (2003) found little NgCAM endocytosis in dendrites and concluded that NgCAM underwent direct delivery. In contrast to NgCAM, Sampo *et al.* (2003) found endocytic VAMP2 vesicles in dendrites and proposed selective retention as its mechanism for maintaining axonal polarity. Our results show that both Golgi-derived and endocytic NgCAM and VAMP2 vesicles exist. Axonal vesicles are Golgi-derived and endocytic proteins in dendrites are targeted to lysosomes and not redirected to the axon. Other membrane proteins have been proposed to reach the axon by transcytosis. In most instances, these endocytosed proteins were not tracked from the dendritic membrane to the axon (Ikonen *et al.*, 1993; de Hoop *et al.*, 1995; Hémar *et al.*, 1997; Garrido *et al.*, 2001; Bel *et al.*, 2009). Even when endocytosed proteins were tracked, the relative contribution of that pathway in comparison to direct delivery was not determined (Yap *et al.*, 2008b; Ascaño *et al.*, 2009; Woodruff *et al.*, 2016; Fletcher-Jones *et al.*, 2019). Therefore, it is possible that transcytosis plays no significant role in maintaining axonal polarity.

### Axonal proteins are sorted at the golgi and in dendritic endosomes

Our findings have implications on the sorting of axonal membrane proteins, which has been a difficult problem (Bonifacino, 2014; Bentley and Banker, 2016; Guardia *et al.*, 2018). We found that axonal membrane proteins can be sorted in two locations, the Golgi apparatus and the dendritic plasma membrane. The primary sorting step takes place at the Golgi apparatus where proteins are loaded into axon-selective vesicles.

These findings allow us to recontextualize previous studies and hint at possible mechanisms for the sorting of axonally polarized membrane proteins. Sorting at the Golgi is likely mediated by heterotetrameric adaptor protein complexes, although the specific interaction is not known. AP-1 and AP-4 are thought to act at the neuronal trans-Golgi (Guardia *et al.*, 2018). In epithelial cells and *Caenorhabditis elegans* neurons, AP-3 also functions at the Golgi (Borgne and Hoflack, 1998; Le Borgne *et al.*, 1998; Nakatsu and Ohno, 2003; Li *et al.*, 2016). The sorting motifs of axonally polarized proteins that are recognized at the Golgi are not yet defined. For NgCAM, the 1142-residue ectodomain may be recognized, as its deletion results in an unpolarized distribution (Sampo *et al.*, 2003). To date, no motif for targeting VAMP2 into axon-selective vesicles has been identified.

The separate sorting event that targets wayward axonal proteins from the dendritic plasma membrane to lysosomes may be mediated by a different heterotetrameric clathrin adaptor complex that participates in endocytosis, AP-2 (Bonifacino, 2014; Robinson, 2015; Guardia *et al.*, 2018; Mettlen *et al.*, 2018). Endocytic signals have been identified in both NgCAM and VAMP2. The cytoplasmic C-terminal domain of NgCAM contains a canonical YxxΦ motif (Kamiguchi *et al.*, 1998; Wisco *et al.*, 2003). Mutation of this motif prevents AP-2-mediated NgCAM endocytosis in the axonal growth cone (Kamiguchi *et al.*, 1998). A loss of the cytoplasmic domain decreases the polarity of cell surface NgCAM (Sampo *et al.*, 2003). After endocytosis, NgCAM associates with other membrane proteins that are constitutively targeted to dendritic lysosomes (Yap *et al.*, 2008b, 2017), in agreement with our findings. Similarly, loss of an endocytic motif in VAMP2 results also in a decrease in polarity (Sampo *et al.*, 2003). These results support the model that both sorting events we identify—at the Golgi for direct delivery to the axon and at the dendritic membrane for targeting to lysosomes—are required for maintaining overall polarity. While outside the scope of this study, future experiments will certainly target each of these sorting events and determine the underlying mechanisms.

### Comparison to previous findings

It is important to consider why our results disagree with conclusions of previous studies. Sampo *et al.* concluded that NgCAM and VAMP2 achieve axonal polarity by different mechanisms (Sampo *et al.*, 2003). These conclusions were based on antibody uptake experiments, in which VAMP2, not NgCAM, was found in dendritic endosomes. We found both proteins in dendritic endosomes, detecting at least twofold more endocytosed VAMP2 than endocytosed NgCAM. Notably, Sampo *et al.* reported a subpopulation of cells with "brightly labeled endocytic [NgCAM] vesicles … in dendrites" (Sampo *et al.*, 2003). It is likely that improvements in imaging technology allowed us to consistently detect this NgCAM population.

Wisco *et al.* concluded that transcytosis was the primary mechanism by which NgCAM reached the axon (Wisco *et al.*, 2003). Compared with ours, these experiments differed fundamentally in their approach by disrupting the endomembrane system for extended periods. In one key experiment, neurons expressing NgCAM were treated with brefeldin A for 12–18 h. After brefeldin A washout, cell surface NgCAM was detected at the dendritic membrane before the axonal membrane. Brefeldin A collapses the secretory pathway into the endoplasmic reticulum (Misumi *et al.*, 1986; Fujiwara *et al.*, 1988; Horton *et al.*, 2005; Bowen *et al.*, 2017; Jensen *et al.*, 2017).

| Construct | Construct design | Accession number (Acc#) | Source |
|---|---|---|---|
| NgCAM-GFP | NgCAM-$_{KLGAPRPT}$-GFP | Z75013 | Adapted from Sampo *et al*. (2003) |
| SBP-NgCAM-GFP | NSS-$_{AYGDLGGSGGGSGGG}$-SBP-$_{GGGSGGGSGGGAS}$-NgCAM-$_{KLGAPRPT}$-GFP | Z75013 | This paper |
| NgCAM-mCherry | NgCAM-$_{KLRILQSTVPRARDPPVV}$-mCherry | Z75013 | This paper |
| NgCAM-HaloTag | NgCAM-$_{KLGAPRPTMASLEPTTEDLYFQSDND}$- HaloTag | Z75013 | (Frank *et al*., 2020) |
| VAMP2-GFP | VAMP2-$_{GDPPVAT}$-GFP | M24105 | Adapted from Sampo *et al*. (2003) |
| VAMP2-GFP-SBP | VAMP2-$_{GDPPVAT}$-GFP-$_{GDLGGSGGGSGGG}$-SBP | M24105 | This paper |
| SigSeq-mCherry | SigSeq-$_{PPVV}$-mCherry | –– | (Kaech *et al*., 2012b) |
| LAMP1-GFP | Lamp1-$_{RG}$-GFP | NM005561 | This paper |

**TABLE 1:** Expression constructs.

In cells that survive long-term brefeldin A treatment, cargo sorting after washout necessarily occurs simultaneously with reformation of the secretory pathway. Such experiments are difficult to interpret because the treatment is prone to disrupt or overwhelm the sorting machinery and may lead to aberrant trafficking. A second key experiment involved the long-term expression of a dominant-negative dynamin. This resulted in fewer cells exhibiting a polarized distribution of NgCAM. Dynamin acts in a wide range of trafficking steps, not exclusively endocytosis (Sever *et al*., 2013; Ramachandran and Schmid, 2018). Blocking membrane fission may prevent anterograde axonal delivery independently of endocytosis. A major strength of our approach is that it minimizes the risk of overloading the secretory pathway and does not rely on manipulations of the trafficking machinery.

Yap *et al*. found that Neep21/Nsg1 depletion moderately decreased the axonal polarity of NgCAM (Yap *et al*., 2008b). In addition to interacting with NgCAM in the early endocytic pathway, which pointed to the model that Nsg1 participates in transcytosis, Nsg1 occupies late endosomes and lysosomes (Yap *et al*., 2017, 2018). These findings are consistent with a model in which Nsg1 targets dendritically endocytosed NgCAM to late endosomes and lysosomes. Therefore, Nsg1 depletion may strand NgCAM at the dendritic plasma membrane, resulting in the moderate decrease of polarity that was observed (Yap *et al*., 2008b). Lysosomes from dendrites can reach the cell body (Yap *et al*., 2018), but our data show that proteins from these do not reach the axon. Future experiments will determine if Nsg1 mediates the lysosomal targeting of other axonal membrane proteins after retrieval from the dendritic plasma membrane.

## MATERIALS AND METHODS

### Cell culture

Primary hippocampal neurons were cultured as previously described (Kaech and Banker, 2006; Kaech *et al*., 2012a,b). E18 rat hippocampi were dissected, trypsinized, dissociated, and plated onto 18-mm glass coverslips coated with poly-L-lysine. Cultured neurons were grown in N2-supplemented MEM and maintained at 37°C with 5% $CO_2$. Stage 4 hippocampal neurons (5–11 DIV) were transfected with Lipofectamine 2000 (Thermo Fisher, Cat# 11668019). Cells were allowed to express for 5–11 h before imaging. This was long enough to produce sufficiently bright vesicle labeling but short enough to reduce buildup of obscurant membrane fluorescence.

### Immunofluorescence

For most immunofluorescence images, neurons were fixed with methanol supplemented with 5 mM EGTA for 11 min at –20°C. To detect endogenous VAMP2 in lysosomes, neurons were fixed with 4% paraformaldehyde (PFA)/0.4% sucrose in phosphate-buffered saline (PBS) for 20 min at 37°C. PFA-treated neurons were permeabilized with 0.5% Triton X-100 in PBS. Neurons were incubated with 0.5% fish skin gelatin in PBS for 1 h to block nonspecific antibody-binding sites. Coverslips were incubated with primary antibodies for 1 h, washed with PBS, incubated with secondary antibodies for 30 min, and mounted on slides with Prolong Diamond Anti-fade (Invitrogen).

Endogenous L1CAM was detected with anti-L1CAM [2C2] (Abcam, Cat#: AB24345); endogenous VAMP2 was detected with anti-Synaptobrevin 2 (Synaptic Systems, Cat#: 104 008).

### DNA constructs

Construct details are described in Table 1. The original NgCAM and VAMP2 constructs were gifts from Gary Banker (Sampo *et al*., 2003). All constructs were confirmed by sequencing.

### SA and lysotracker labeling

Neurons were incubated in conditioned medium containing 18.5 μM of SA conjugated to Alexa Fluor 555 (Thermo Fisher, Cat#: S21381). After a 30-min incubation, unbound SA was removed by briefly rinsing cells twice with warmed, conditioned, SA-free medium. Control cells not subjected to SA incubation were rinsed in the same way. For lysotracker experiments, 10 nM lysotracker deep red (Thermo Fisher, Cat#: L12492) was added to incubating cells 3 min before rinsing. Washed coverslips were then loaded into a prewarmed imaging chamber, submerged in Hibernate E medium without phenol red (Brain-Bits), and transferred to the microscope for imaging.

### Imaging

Most images and all movies were acquired with an Andor Dragonfly built on a Ti2 (Nikon) with a CFI Apo 60× 1.49 objective (Nikon) and two sCMOS cameras (Zyla 4.2+; Andor). The imaging stage, microscope objectives, and cell sample were kept at 37°C in a warmed enclosure (full lexan incubation ensemble; OkoLab). The *z*-axis movement was controlled by the Perfect Focus System on the Ti-E microscope (Nikon). Live movies were recorded for 30 s at two frames per second. Axons were identified with an anti-neurofascin antibody (NeuroMab, Cat#: 75-027) conjugated to CF405 (Mix-n-Stain CF405S Antibody Labeling Kit; Biotum, Cat#: 92231) in the imaging medium.

SA uptake experiments (Figure 2, C–E) were acquired using a Zeiss Axio Imager Z1 microscope (Carl Zeiss) equipped with an Axiocam 506 mono.

### Analysis

MetaMorph Image Analysis Software (Molecular Devices) was used to generate kymographs of vesicle transport from movies. A single analyst manually identified all transport events from kymographs. To ensure consistency and reduce bias, multiple experiments and conditions were combined into a large dataset and the analyst was blinded to the cell and fluorophore channel of origin for each kymograph. Each continuous line with a constant slope was scored as a single transport event. A single vesicle could undergo multiple transport events if there was a distinct pause between them. Once all event coordinates had been identified, overlapping events were determined by visually comparing the locations, slopes, and run lengths of events from each channel. Only events that demonstrated substantial overlap were scored.

Event coordinates were exported to Microsoft Excel or GraphPad Prism for analysis. Event velocities and run lengths (distance moved along the long axis of the neurite) were calculated. To ensure only microtubule-based long-range transport events were included in the analysis, excursions <3 µm were excluded. The number of events per 100 µm was defined as the total number of events recorded normalized to the total length of neurite analyzed for all cells in a treatment. Vesicle fluorescence intensity was quantified by measuring the intensity of each fluorescent transport event after subtraction of background camera fluorescence. Percentage overlap was calculated as the number of overlapping events divided by the total number of observed events. Run lengths plotted as histograms were fit to a single-exponential decay to determine mean run length:

$$y = y_0 + A^{\left(\frac{-x}{l}\right)}$$

where $A$ is the maximum amplitude, and $l$ is the mean run length reported as ±SEM.

GFP and SA555 fluorescence intensities were analyzed using Image J. Lysosomal overlap was quantified using Image J with Cell Counter plug-in. *P* values were determined by Welch's *t* test (Figures 2D; 4, C and E; and 5, C, E, and I), one-way ANOVA (Figures 2G and 3, B–E), or Kolmogrov-Smirnov test (Figures 4D and 5D). Error bars show SEM (Figures 2G; 4C; 5C; and 6, C, D, F, and G) or SD (Figures 3, B–E; 4, G and H; and 5, G and H). Between 12 and 61 cells were evaluated for each experiment, including cells from at least two independent cultures in all treatments.

## ACKNOWLEDGMENTS

We thank Geraldine Quinones for excellent technical assistance in culturing and maintaining hippocampal neurons. We thank Susan Gilbert, Gary Banker, Ines Hahn, André Völtzman, Catherine Drerup, and members of the Bentley lab for their helpful comments on the paper. We thank the BioResearch facility at Rensselaer for assistance with husbandry and tissue collection. This work was supported by National Institutes of Health (NIH) Grant MH066179 and an NIH-funded predoctoral fellowship to A.T.N. (T32GM067545).

## REFERENCES

Ahmari SE, Buchanan JA, Smith SJ (2000). Assembly of presynaptic active zones from cytoplasmic transport packets. Nat Neurosci 3, 445–451.

Akin EJ, Solé L, Dib-Hajj SD, Waxman SG, Tamkun MM (2015). Preferential targeting of Nav1.6 voltage-gated Na+ channels to the axon initial segment during development. PLoS One 10, 1–18.

Al-Bassam S, Xu M, Wandless TJ, Arnold DB (2012). Differential trafficking of transport vesicles contributes to the localization of dendritic proteins. Cell Rep 2, 89–100.

Ascaño M, Richmond A, Borden P, Kuruvilla R, Ascano M, Richmond A, Borden P, Kuruvilla R (2009). Axonal targeting of Trk receptors via transcytosis regulates sensitivity to neurotrophin responses. J Neurosci 29, 11674–11685.

Bel C, Oguievetskaia K, Pitaval C, Goutebroze L, Faivre-Sarrailh C (2009). Axonal targeting of Caspr2 in hippocampal neurons via selective somatodendritic endocytosis. J Cell Sci 122, 3403–3413.

Bentley M, Banker G (2016). The cellular mechanisms that maintain neuronal polarity. Nat Rev Neurosci 17, 611–622.

Bonifacino JS (2014). Adaptor proteins involved in polarized sorting. J Cell Biol 204, 7–17.

Le Borgne R, Alconada A, Bauer U, Hoflack B (1998). The mammalian AP-3 adaptor-like complex mediates the intracellular transport of lysosomal membrane glycoproteins. J Biol Chem 273, 29451–29461.

Borgne RLe, Hoflack B (1998). Mechanisms of protein sorting and coat assembly: Insights from the clathrin-coated vesicle pathway. Curr Opin Cell Biol 10, 499–503.

Bowen AB, Bourke AM, Hiester BG, Hanus C, Kennedy MJ (2017). Golgi-independent secretory trafficking through recycling endosomes in neuronal dendrites and spines. Elife 6, 1–27.

Burack MA, Silverman MA, Banker G (2000). The role of selective transport in neuronal protein sorting. Neuron 26, 465–472.

Caceres A, Banker G, Steward O, Binder L, Payne M (1984). MAP2 is localized to the dendrites of hippocampal neurons which develop in culture. Dev Brain Res 13, 314–318.

Das U, Scott DA, Ganguly A, Koo EH, Tang Y, Roy S (2013). Activity-induced convergence of app and bace-1 in acidic microdomains via an endocytosis-dependent pathway. Neuron 79, 447–460.

Das U, Wang L, Ganguly A, Saikia JM, Wagner SL, Saikia JM, Koo EH, Roy S (2015). Visualizing APP and BACE-1 approximation in neurons yields insight into the amyloidogenic pathway. Nat Neurosci 19, 55–64.

Farías GG, Cuitino L, Guo X, Ren X, Jarnik M, Mattera R, Bonifacino JS (2012). Signal-mediated, AP-1/clathrin-dependent sorting of transmembrane receptors to the somatodendritic domain of hippocampal neurons. Neuron 75, 810–823.

Farías GG, Guardia CM, De Pace R, Britt DJ, Bonifacino JS (2017). BORC/kinesin-1 ensemble drives polarized transport of lysosomes into the axon. Proc Natl Acad Sci USA 114, E2955–E2964.

Fletcher-Jones A, Hildick KL, Evans AJ, Nakamura Y, Wilkinson KA, Henley JM (2019). The C-terminal helix 9 motif in rat cannabinoid receptor type 1 regulates axonal trafficking and surface expression. eLife 8, e44252.

Frank M, Citarella CG, Quinones GB, Bentley M (2020). A novel labeling strategy reveals that myosin Va and myosin Vb bind the same dendritically polarized vesicle population. Traffic.

Fujiwara T, Oda K, Yokota S, Takatsuki A, Ikehara Y (1988). Brefeldin A causes disassembly of the Golgi complex and accumulation of secretory proteins in the endoplasmic reticulum. J Biol Chem 263, 18545–18552.

Ganguly A, Han X, Das U, Wang L, Loi J, Sun J, Gitler D, Caillol G, Leterrier C, Yates JR, Roy S (2017). Hsc70 chaperone activity is required for the cytosolic slow axonal transport of synapsin. J Cell Biol 216, 2059–2074.

Ganguly A, Tang Y, Wang L, Ladt K, Loi J, Dargent B, Leterrier C, Roy S (2015). A dynamic formin-dependent deep F-actin network in axons. J Cell Biol 210, 401–417.

Garrido JJ, Fernandes F, Giraud P, Mouret I, Pasqualini E, Fache MP, Jullien F, Dargent B (2001). Identification of an axonal determinant in the C-terminus of the sodium channel Nav1.2. EMBO J 20, 5950–5961.

Goo MS, Sancho L, Slepak N, Boassa D, Deerinck TJ, Ellisman MH, Bloodgood BL, Patrick GN (2017). Activity-dependent trafficking of lysosomes in dendrites and dendritic spines. 216, 2499–2513.

Grimm JB, English BP, Chen J, Slaughter JP, Zhang Z, Revyakin A, Patel R, Macklin JJ, Normanno D, Singer RH, *et al.* (2015). A general method to improve fluorophores for live-cell and single-molecule microscopy. Nat Methods 12, 244–250.

Grumet M (1992). Structure, expression, and function of Ng-CAM, a member of the immunoglobulin superfamily involved in neuron-neuron and neuron-glia adhesion. J Neurosci Res 31, 1–13.

Guardia CM, De Pace R, Mattera R, Bonifacino JS (2018). Neuronal functions of adaptor complexes involved in protein sorting. Curr Opin Neurobiol 51, 103–110.

Gumy LF, Hoogenraad CC (2018). Local mechanisms regulating selective cargo entry and long-range trafficking in axons. Curr Opin Neurobiol 51, 23–28.

Gumy LF, Katrukha EA, Grigoriev I, Jaarsma D, Kapitein LC, Akhmanova A, Hoogenraad CC (2017). MAP2 defines a pre-axonal filtering zone to regulate KIF1- versus KIF5-dependent cargo transport in sensory neurons. Neuron 94, 347–362.e7.

Hedstrom KL, Ogawa Y, Rasband MN (2008). AnkyrinG is required for maintenance of the axon initial segment and neuronal polarity. J Cell Biol 183, 635–640.
Hémar A, Olivo J-C, Williamson E, Saffrich R, Dotti CG (1997). Dendroaxonal transcytosis of transferrin in cultured hippocampal and sympathetic neurons. J Neurosci 17, 9026–9034.
Hoo LS, Banna CD, Radeke CM, Sharma N, Albertolle ME, Low SH, Weimbs T, Vandenberg CA (2016). The SNARE protein syntaxin 3 confers specificity for polarized axonal trafficking in neurons. PLoS One 11, 1–20.
de Hoop M, von Poser C, Lange C, Ikonen E, Hunziker W, Dotti CG (1995). Intracellular routing of wild-type and mutated polymeric immunoglobulin receptor in hippocampal neurons in culture. J Cell Biol 130, 1447–1459.
Horton AC, Ehlers MD (2003). Neuronal Polarity and Trafficking. Neuron 40, 277–295.
Horton AC, Rácz B, Monson EE, Lin AL, Weinberg RJ, Ehlers MD (2005). Polarized secretory trafficking directs cargo for asymmetric dendrite growth and morphogenesis. Neuron 48, 757–771.
Huang CYM, Rasband MN (2018). Axon initial segments: structure, function, and disease. Ann N Y Acad Sci 1420, 46–61.
Ikonen E, Parton RG, Hunziker W, Simons K, Dotti CG (1993). Transcytosis of the polymeric immunoglobulin receptor in cultured hippocampal neurons. Curr Biol 3, 635–644.
Jareb M, Banker G (1998). The Polarized Sorting of Membrane Proteins Expressed in Cultured Hippocampal Neurons Using Viral Vectors. Neuron 20, 855–867.
Jenkins B, Decker H, Bentley M, Luisi J, Banker G (2012). A novel split kinesin assay identifies motor proteins that interact with distinct vesicle populations. J Cell Biol 198, 749–761.
Jensen CS, Watanabe S, Rasmussen HB, Schmitt N, Olesen SP, Frost NA, Blanpied TA, Misonou H (2014). Specific sorting and post-golgi trafficking of dendritic potassium channels in living neurons. J Biol Chem 289, 10566–10581.
Jensen CS, Watanabe S, Stas JI, Klaphaak J, Yamane A, Schmitt N, Olesen SP, Trimmer JS, Rasmussen HB, Misonou H (2017). Trafficking of Kv2.1 channels to the axon initial segment by a novel nonconventional secretory pathway. J Neurosci 37, 11523–11536.
Kaech S, Banker G (2006). Culturing hippocampal neurons. Nat Protoc 1, 2406–2415.
Kaech S, Huang C-F, Banker G (2012a). General considerations for live imaging of developing hippocampal neurons in culture. Cold Spring Harb Protoc 3, 312–318.
Kaech S, Huang C-F, Banker G (2012b). Short-term high-resolution imaging of developing hippocampal neurons in culture. Cold Spring Harb Protoc 3, 340–343.
Kamiguchi H, Long KE, Pendergast M, Schaefer AW, Rapoport I, Kirchhausen T, Lemmon V (1998). The neural cell adhesion molecule L1 interacts with the AP-2 adaptor and is endocytosed via the clathrin-mediated pathway. J Neurosci 18, 5311–5321.
Keefe AD, Wilson DS, Seelig B, Szostak JW (2001). One-step purification of recombinant proteins using a nanomolar-affinity streptavidin-binding peptide, the SBP-tag. Protein Expr Purif 23, 440–446.
Koppers M, Farías GG (2021). Organelle distribution in neurons: Logistics behind polarized transport. Curr Opin Cell Biol 71, 46–54.
Lasiecka ZM, Winckler B (2011). Mechanisms of polarized membrane trafficking in neurons - Focusing in on endosomes. Mol Cell Neurosci 48, 278–287.
Leterrier C (2018). The axon initial segment: an updated viewpoint. J Neurosci 38, 1922–17.
Leterrier C, Dargent B (2014). No Pasaran! Role of the axon initial segment in the regulation of protein transport and the maintenance of axonal identity. Semin Cell Dev Biol 27, 44–51.
Leterrier C, Dubey P, Roy S (2017). The nano-architecture of the axonal cytoskeleton. Nat Rev Neurosci 18, 713–726.
Lewis TL, Mao T, Arnold DB (2011). A role for Myosin VI in the localization of axonal proteins. PLoS Biol 9, e1001021.
Li P, Merrill SA, Jorgensen EM, Shen K (2016). Two clathrin adaptor protein complexes instruct axon-dendrite polarity. Neuron 90, 564–580.
Liu JSS, Schubert CRR, Fu X, Fourniol FJJ, Jaiswal JKK, Houdusse A, Stultz CMM, Moores CAA, Walsh CAA (2012). Molecular basis for specific regulation of neuronal kinesin-3 motors by doublecortin family proteins. Mol Cell 47, 707–721.
McCann CM, Bareyre FM, Lichtman JW, Sanes JR (2005). Peptide tags for labeling membrane proteins in live cells with multiple fluorophores. Biotechniques 38, 945–952.
El Meskini R, Jin L, Marx R, Bruzzaniti A, Lee J, Emeson RB, Mains RE (2001). A signal sequence is sufficient for green fluorescent protein to be routed to regulated secretory granules. Endocrinology 142, 864–873.
Mettlen M, Chen P, Srinivasan S, Danuser G, Schmid SL (2018). Regulation of clathrin-mediated endocytosis. Annu Rev Biochem 87, 871–896.
Misumi Y, Misumi Y, Miki K, Takatsuki A, Tamura G, Ikehara Y (1986). Novel blockade by brefeldin A of intracellular transport of secretory proteins in cultured rat hepatocytes. J Biol Chem 261, 11398–11403.
Morag E, Bayer EA, Wilchek M (1996). Reversibility of biotin-binding by selective modification of tyrosine in avidin. Biochem J 316, 193–199.
Nabb AT, Frank M, Bentley M (2020). Smart motors and cargo steering drive kinesin-mediated selective transport. Mol Cell Neurosci 103, 103464.
Nakatsu F, Ohno H (2003). Adaptor protein complexes as the key regulators of protein sorting in the post-Golgi network. Cell Struct Funct 28, 419–429.
Petersen JD, Kaech S, Banker G (2014). Selective microtubule-based transport of dendritic membrane proteins arises in concert with axon specification. J Neurosci 34, 4135–4147.
Radler MR, Suber A, Spiliotis ET (2020). Spatial control of membrane traffic in neuronal dendrites. Mol Cell Neurosci 105, 103492.
Ramachandran R, Schmid SL (2018). The dynamin superfamily. Curr Biol 28, R411–R416.
Robinson MS (2015). Forty years of clathrin-coated vesicles. Traffic 16, 1210–1238.
Sampo B, Kaech S, Kunz S, Banker G (2003). Two distinct mechanisms target membrane proteins to the axonal surface. Neuron 37, 611–624.
Sankaranarayanan S, Ryan TA (2000). Real-time measurements of vesicle-SNARE recycling in synapses of the central nervous system. Nat Cell Biol 2, 197–204.
Sever S, Chang J, Gu C (2013). Dynamin rings: Not just for fission. Traffic 14, 1194–1199.
Silverman MA, Kaech S, Jareb M, Burack MA, Vogt L, Sonderegger P, Banker G (2001). Sorting and directed transport of membrane proteins during development of hippocampal neurons in culture. Proc Natl Acad Sci USA 98, 7051–7057.
Sollner T, Whiteheart SW, Brunner M, Erdjument-bromage H, Geromanos S, Tempst P, Rothman JE (1993). SNAP receptors implicated in vesicle targeting and fusion. Nature 362, 318–324.
Trimble WS (1993). Analysis of the structure and expression of the VAMP family of synaptic vesicle proteins. J Physiol Paris 87, 107–115.
Winckler B, Mellman I (1999). Neuronal polarity: Controlling the sorting and diffusion of membrane components. Neuron 23, 637–640.
Wisco D, Anderson ED, Chang MC, Norden C, Boiko T, Fölsch H, Winckler B (2003). Uncovering multiple axonal targeting pathways in hippocampal neurons. J Cell Biol 162, 1317–1328.
Woodruff G, Reyna SM, Dunlap M, Van Der Kant R, Callender JA, Young JE, Roberts EA, Goldstein LSB (2016). Defective transcytosis of APP and lipoproteins in human iPSC-derived neurons with familial Alzheimer's disease mutations. Cell Rep 17, 759–773.
Yamamoto H, Demura T, Morita M, Banker GA, Tanii T, Nakamura S (2012). Differential neurite outgrowth is required for axon specification by cultured hippocampal neurons. J Neurochem 123, 904–910.
Yang R, Bostick Z, Garbouchian A, Luisi J, Banker G, Bentley M (2019). A novel strategy to visualize vesicle-bound kinesins reveals the diversity of kinesin-mediated transport. Traffic, 851–866.
Yap CC, Digilio L, McMahon LP, Garcia ADR, Winckler B (2018). Degradation of dendritic cargos requires Rab7-dependent transport to somatic lysosomes. J Cell Biol 217, 3141–3159.
Yap CC, Digilio L, McMahon L, Winckler B (2017). The endosomal neuronal proteins Nsg1/NEEP21 and Nsg2/P19 are itinerant, not resident proteins of dendritic endosomes. Sci Rep 7, 1–17.
Yap CC, Nokes RL, Wisco D, Anderson E, Fölsch H, Winckler B (2008a). Pathway selection to the axon depends on multiple targeting signals in NgCAM. J Cell Sci 121, 1514–1525.
Yap CC, Wisco D, Kujala P, Lasiecka ZM, Cannon JT, Chang MC, Hirling H, Klumperman J, Winckler B (2008b). The somatodendritic endosomal regulator NEEP21 facilitates axonal targeting of L1/NgCAM. J Cell Biol 180, 827–842.